High-Power 4H-SiC JBS Rectifiers

Ranbir Singh, D. Craig Capell, Allen R. Hefner, *Fellow, IEEE*, Jason Lai, *Senior Member, IEEE*, and John W. Palmour, *Member, IEEE*

***Abstract*—This paper reports the detailed design, fabrication, and characterization of two sets of high-power 4H-Silicon Carbide (4H-SiC) Junction Barrier Schottky (JBS) diodes—one with a 1500-V, 4-A capability and another with 1410-V, 20-A capability. Two-dimensional (2-D) device simulations show that a grid spacing of 4 μm results in the most optimum trade-off between the on-state and off-state characteristics for these device ratings. JBS diodes with linear and honeycombed p^+ grids, Schottky diodes and implanted p-i-n diodes fabricated alongside show that while 4H-SiC JBS diodes behave similar to Schottky diodes in the on-state and switching characteristics, they show reverse characteristics similar to p-i-n diodes. Measurements on 4H-SiC JBS diodes indicate that the reverse-recovery time (τ_{rr}) and associated losses are near-zero even at a high reverse dI/dt of 75 A/μs. A dc/dc converter efficiency improvement of 3–6% was obtained over the fastest, lower blocking voltage silicon (Si) diode when operated in the 100–200 kHz range. The 1410-V/20-A JBS diodes were evaluated for both hard- and soft-switching applications. Experimental results indicate that their conduction characteristics are comparable with the Si diode counterpart, but the switching characteristics are far superior. When applied to hard-switching choppers, it reduces not only the reverse-recovery loss, but also the main switch turn-on loss. Using the MOSFET as the main switching device, the combination of switch turn-on loss and diode reverse-recovery loss shows more than a 60% reduction. When applied to soft-switching choppers, the SiC JBS diode is used as the auxiliary diode to avoid the voltage spike during auxiliary branch turn-off. With the conventional ultrafast reverse-recovery Si diode, a voltage spike exceeds the switched-voltage transition by 100% and the auxiliary circuit requires additional voltage clamping or snubbing to avoid over-voltage failure. With the SiC JBS diode, however, the voltage spike is reduced to less than 50% of the switched-voltage transition and the additional voltage clamping circuit can be eliminated. Savings in soft-switching choppers using SiC JBS diodes can be realized in size and weight reduction, energy loss reduction, and reduced packaging complexity.**

***Index Terms*—Junction Barrier Schottky (JBS), merged p-i-n Schottky, rectifier, reverse-recovery, Schottky, silicon carbide (SiC), ultrafast diodes.**

I. Introduction

POWER devices made with silicon carbide (SiC) are expected to show great performance advantages as compared to those made with other semiconductors. This is primarily because 4H-SiC has an order of magnitude higher breakdown electric field (2–4 $\times 10^6$ V/cm) than Si and GaAs and an electron mobility only $\sim 20\%$ lower than Si. A high breakdown electric field allows the design of SiC power devices with thinner and higher doped voltage-blocking layers. 4H-SiC unipolar devices are expected to replace Si bipolar switches and rectifiers in the 600–3000 V range in the future. Generally speaking, there are three classes of power rectifiers:

1) Schottky diodes, which offer extremely high switching speed but suffer from lower blocking voltage and high leakage current;
2) p-i-n diodes, which offer high-voltage operation and low-leakage current, but show reverse-recovery charge during switching;
3) Junction Barrier Schottky (JBS) diodes, which offer Schottky-like on-state and switching characteristics and p-i-n-like off-state characteristics.

In conventional high-voltage ($>$ 600 V) circuits using Si p-i-n diodes, the primary source of power loss is the dissipation of reverse-recovery charge during the turn-off of the rectifier. The switches used in these inverter and converter circuits have to be de-rated substantially to account for this large heat dissipation. The 4H-SiC JBS diode offers nearly zero reverse-recovery charge. This allows the design of packages with much lower thermal dissipation requirements for both the rectifier and the switch. The on-state performance of a 4H-SiC JBS diode is expected to be comparable to that of a Si p-i-n diode. The on-state voltage drop at sufficiently high current densities for a unipolar device (like Schottky/JBS diode) depends on the resistive voltage drop in the low-doped drift region. To achieve a high blocking voltage, the drift region doping must be reduced and its thickness must be increased. This leads to a high on-state voltage drop for a high-voltage unipolar device. In the case of a bipolar device (like p-i-n diode), minority carrier injection into the low-doped drift region during on-state operation results in very low voltage drop even for very high breakdown voltage rated devices. However, in the case of a bipolar device, the device does not turn ON until a forward bias equivalent to the bandgap of the device is applied. Therefore, the breakdown voltage rating for which the on-state performance of a p-i-n diode (a bipolar device) is superior to that of a Schottky/JBS diode (a unipolar device) for equivalent sized die depends on the material used for its fabrication. For Si, this limit is approximately 200 V; for GaAs, it is approximately 500 V; and for 4H-SiC it is approximately 3000 V.

II. Basic Operation and Design of 4H-SiC JBS Diodes

A cross section of a 4H-SiC JBS rectifier operating in the forward and reverse bias is shown in Fig. 1. A JBS diode consists

Manuscript received March 15, 2002; revised August 30, 2002. This work was supported by the Defense Advanced Research Projects Agency's (DARPA's) MEGAWATT Program under Office of Naval Research Contract N00014-98-C-0191, monitored by G. Campisi and D. Radack. Contributions of the National Institute of Standards and Technology are not subject to U.S. copyright. The review of this paper was arranged by Editor M. A. Shibib.

R. Singh, D. C. Capell, and J. W. Palmour are with Cree Inc., Durham NC 27703 USA (e-mail: ranbir_singh@cree.com).

A. R. Hefner is with the National Institute of Standards and Technology (NIST), Gaithersburg, MD 20899 USA.

J. Lai is with the Virginia Polytechnic Institute and State University, CPES, Blacksburg, VA 24061-0111 USA.

Digital Object Identifier 10.1109/TED.2002.804715

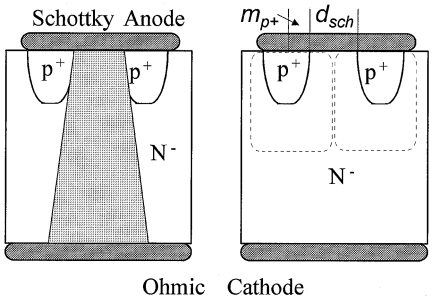

Fig. 1. On-state current flows through the Schottky anode while reverse leakage is limited by depletion from adjacent p^+ grids in a JBS diode.

of interdigitated Schottky and p^+ implanted areas. For on-state drops of < 3 V, only the Schottky regions of the diode conduct. The on-state voltage drop ($\boldsymbol{V}_F$) of the device is determined by the resistance of the drift region (which is the primary source of $\boldsymbol{V}_F$ at operating current density), metal-SiC barrier height of the Schottky metal, and the relative area of the Schottky versus the p^+ implanted regions. It is important to achieve a good quality Schottky interface for a low on-state voltage drop JBS diode. Since the Schottky regions of the diode have to compensate for the non-conducting p^+ grid area of the JBS diode, the current density in the Schottky regions of the diode exceeds the current density of the entire device. The presence of the p^+ implanted regions give a high surge current, dV/dt and dI/dt rating, since the heat produced by the voltage drop is relatively small when a high current density flows through the device. This is because minority carrier injection results at the p^+n^- junctions when very high current densities are flowing through the device. The Schottky contacts to the drift region provide an effective shunt for the extraction of minority carriers when the device recovers from such high current density transients.

The metal-SiC barrier height of the Schottky metal should be low enough to give a low on-state voltage, but high enough to effectively block voltage during the off-state. As the reverse bias increases, the depletion regions from adjacent p^+ implanted regions pinchoff the leakage current arising from the Schottky contacts of the device. The leakage current in the Schottky regions occurs due to Schottky barrier lowering at the metal-n^- junction. The presence of the p^+ implanted regions reduces the electric field at the metal-SiC junction because of two-dimensional (2-D) charge sharing. This property is especially useful when the diode is operating at elevated temperatures since the effect of Schottky barrier lowering is enhanced with increasing temperature.

Early work on SiC JBS diodes concentrated on the design and fabrication of relatively low voltage (i.e., $<$ 1 kV) devices. The design parameters for the design of JBS diodes in this voltage range have somewhat different values as compared to higher voltage devices. Held *et al.* [1] presented detailed design, simulations and experimental results on 700-V, 1-A JBS diodes. Dahlquist *et al.* [2] have also shown JBS diodes in both 4H- and 6H-SiC. In addition to data on these two polytypes, a study on the variation of p^+ spacing shows that the blocking voltage obtained depends on this parameter. On 1-kV devices, a specific on-state resistance of 19 mΩ-cm^2 were presented. Recent results have shown considerably higher currents [3] and higher temperature [4] operation. Paralleling many individual chips formed these 140-A, 800-V modules. JBS diodes are attractive in the higher voltage (1 kV–3 kV) range because many demonstrations of Schottky diodes recently have shown acceptable performance and ratings in the $<$ 1 kV range [5]. The following section describes the design and fabrication of diodes with a $>$ 1.4 kV ratings.

A. JBS Parameter Optimization Using 2–D Simulations

The rectifiers reported here were made using 20 μm thick epitaxial layers with a donor doping concentration of 2E15 cm^{-3} on 4H-SiC n^+ substrates. There exists a fundamental trade-off between the $\boldsymbol{V}_F$ and leakage current of the JBS diode. The design parameters that affect this trade-off are

1) the relative area of the p^+ implanted region;
2) the geometrical layout of the p^+ implanted region.

A large p^+ implanted area is expected to result in a higher $\boldsymbol{V}_F$ because of the smaller conducting area, but may offer lower leakage due to a more effective pinchoff of the Schottky portion. As shown in Fig. 1, the portion of the Anode metal that contacts the n^- epitaxial layer (Schottky diode portion of the device) is called $d_{\rm sch}$ and m_{p^+} is half the total metal-implanted p^+ contact width with Anode metal.

To optimize the design parameters $d_{\rm sch}$ and m_{p^+}, detailed 2-D device simulations were performed at a nominal cell current density of 200 A/cm^2 in the on-state and 2000 V in the off-state. The three values for $d_{\rm sch}$ analyzed were 2 μm, 4 μm, and 10 μm. For the on-state simulations, the localized peak current density at the Schottky region edges obtained for $d_{\rm sch} = 2$ μm was 1200 A/cm^2; for $d_{\rm sch} = 4$ μm was 670 A/cm^2; and for $d_{\rm sch} = 10$ μm was 570 A/cm^2. While the V_F for the case of $d_{\rm sch} = 2$ μm is significantly higher (2.75 V), the difference between the V_F at $d_{\rm sch} = 4$ μm (2.45 V) and $d_{\rm sch} = 10$ μm (2.42 V) is negligible. As expected, simulations show that the V_F increases as m_{p^+} is increased from 1 μm to 3 μm. Since it is fairly straight forward to make a 2 μm (corresponding to $m_{p^+} = 1$ μm) p^+ implanted region using standard photolithography techniques, this value was chosen for the fabrication of JBS diodes. To evaluate the effectiveness of $d_{\rm sch}$ on the reverse bias operation (at 2000 V) of the JBS diode, the ratio of electric field at the Schottky interface to the peak electric field (at the bottom of the p^+ region) was analyzed using device simulations. It was found that the peak electric field at the Schottky interface is only 62% of the peak electric field for $d_{\rm sch} = 4$ μm, but increases significantly to 80% for $d_{\rm sch} = 10$ μm. For $d_{\rm sch} = 2$ μm, this ratio is 57%. From these simulation results, it can be concluded that a p^+ region spacing of 4 μm is optimum for the fabrication of these 2-kV SiC JBS diodes.

III. Design and Fabrication of First Batch of JBS Diodes

The purpose of the first batch of devices reported here was to implement and evaluate various designs to determine which JBS diode design was the most suitable for the fabrication of larger and better optimized devices using a given set of available fabrication techniques.

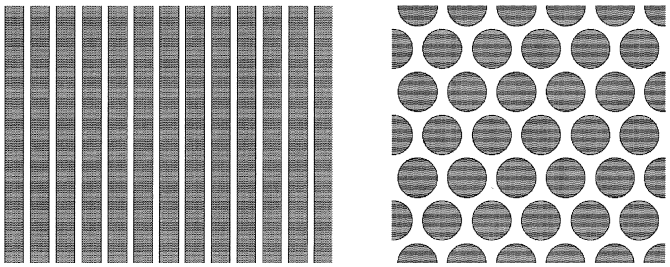

(a) (b)

Fig. 2. The p^+ grid layout designs for JBS diodes: (a) linear grid design and (b) honeycomb grid designs.

A. JBS Layout Designs of p^+ Grid

An important aspect of the design of the JBS diode is the geometric layout of the grid for a given area of the p^+ implanted region. Two extreme examples of the p^+ layout are the linear grid [see Fig. 2(a)] and the honeycomb grid [see Fig. 2(b)]. The shaded regions correspond to the unimplanted areas, while the clear regions are the p^+ implanted regions. Since the honeycombed design offers a more effective pinchoff of the leakage current, a wider unimplanted region can be expected to deliver an identical leakage current as compared to the linear grid design. On the other hand, the larger p^+ implanted area inherent in the honeycomb design is wasted diagonally across Schottky areas (in the middle of the triangle of unimplanted regions) for a given distance between adjacent Schottky regions. In order to compare the performance of JBS diodes, it is essential to fabricate Schottky and p-i-n diodes on the same wafer. Hence, for the first batch of devices, four kinds of devices were placed on the same mask: 1) honeycomb JBS diode; 2) linear JBS diode; 3) implanted p-i-n diode; and 4) pure Schottky diodes. All of these diodes had an identical junction termination extension (JTE) design in order to reduce the electric field at the device edges during the reverse bias operation. The length of the JTE length was fixed at 50 μm.

B. JBS Diode Fabrication

The fabrication sequence of these diodes is as follows: Aluminum was implanted at a high temperature to form the p^+ grid of JBS diodes and anode of the p-i-n diodes. An optimum dose of boron was used to implement the JTE edge termination resulting in a targeted active acceptor concentration of 7×10^{12} cm^{-2}. These implants were annealed at 1625 °C in Si over-pressure followed by a thick LPCVD SiO_2 deposition. Thereafter, Ni deposition and ohmic anneal were performed to form the p-i-n anode and backside cathode contacts. A Ni evaporation step was used to form the Anodes of the JBS as well as the Schottky diodes, followed by a 2-μm Ti/Pt/Au deposition on top and bottom of the wafer to reduce the spreading resistance.

C. Static Characteristics

Fig. 3 shows the comparison of on-state $J-V$ characteristics of typical Schottky, linear JBS, honeycomb JBS, and p-i-n diodes fabricated in this batch of devices. The on-state characteristics of the linear JBS and Schottky diodes are almost identical, indicating excellent current spreading and

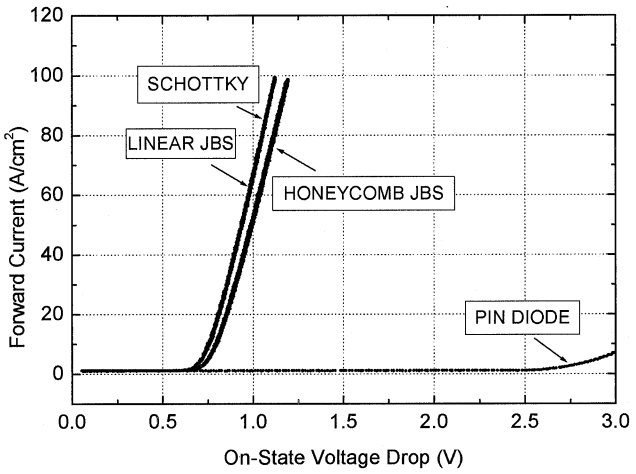

Fig. 3. Measured on-state $J-V$ comparison of 1.5 mm $\times$ 1.5 mm Schottky, linear JBS, honeycomb JBS, and p-i-n diodes fabricated on the same wafer.

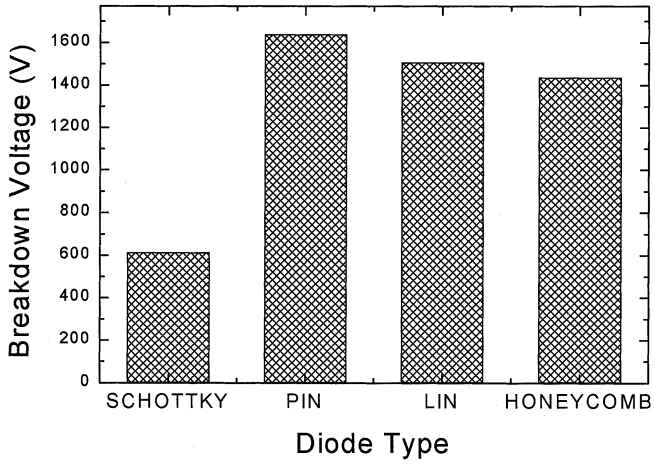

Fig. 4. Blocking voltage comparison for Schottky, p-i-n, linear JBS, and honeycomb JBS diodes fabricated on the same wafer.

minimal increase in the $\boldsymbol{V}_F$ due to the introduction of the p^+ implanted grid. The honeycomb diodes suffer from a slightly higher on-state voltage drop than linear grid diodes. At a forward current of 4 A (200 A/cm^2) on the linear JBS diode, an on-state voltage drop ($\boldsymbol{V}_F$) of 3.1 V was obtained on some "best few" devices. This corresponds to a specific on-resistance of 10.5 mΩ-cm^2. An ideality factor of 1.07 was measured on this diode. The slightly non-ideal on-state behavior of p-i-n diodes was probably caused by damage caused by a high-dose Aluminum ion implantation used for the formation of the anode regions. The reverse bias characteristics of the honeycomb JBS and linear JBS diodes are much more similar to the p-i-n diodes than to the Schottky diodes. At a leakage current of 50 μA, the blocking voltage of typical good Schottky, honeycomb JBS, linear JBS, and p-i-n diodes were measured at 610 V, 1380 V, 1480 V, and 1980 V, respectively, as shown in Fig. 4. This leakage current corresponds to a current density of only 3×10^{-4} A/cm^2. The highest voltage 4-A JBS diode (linear grid design) had a blocking voltage of 1500 V. *Based on these experimental results, only a linear grid JBS diode was implemented in the second batch of higher voltage, higher current JBS diodes, reported later in this paper.*

D. Dynamic Characteristics of 4H-SiC JBS Diodes

Detailed switching measurements were conducted on some 1200-V blocking 4H-SiC JBS diodes from the same wafer that yielded the 1500-V device to test the reverse-recovery currents and the impact of JBS diodes on a standard dc/dc converter [6]. These small area (0.0045 cm^2) diodes had a low current rating of 0.5 A (111 A/cm^2). In addition, electromagnetic interference (EMI) signatures were recorded on the dc/dc converter for Si and SiC diodes.

1) Reverse-Recovery Measurements: The test circuit used for characterizing the diodes for reverse-recovery used the diode under test (DUT) in a boost configuration [6]. A 5-cycle burst current built through an inductor and measurements were made during the last cycle of the burst. A 6LF6 vacuum tube was used as a switch in place of the usual MOSFET switch to achieve low parasitic capacitance at the anode of the DUT and extremely fast switching speed. A resistor isolated the DUT from the parasitic capacitance of the inductor and also was used to quickly reset the inductor current to zero after each 5-cycle test burst so that the DUT was not heated. The dV/dt for the square-wave drive burst to the tube could be adjusted to achieve different dI/dt values for the DUT. Varying the value of dV/dt makes it easier to identify the portion of the diode recovery due to charge storage and the portion due to device capacitance. Adding values of capacitance to the output of the tube emulates the conditions of using anti-parallel switching devices of different output capacitance in an application circuit. The turn-off characteristics of the JBS diodes were measured for many different dI/dt values. Data obtained thus showed that even for the fastest turn-off, the recovery of the SiC diode is mostly capacitive in nature. This capacitance was calculated to be 3.3 pF when the reverse voltage was several hundred volts and this value is consistent with the junction depletion capacitance value calculated using the blocking region doping concentration. In contrast, the bulk of the reverse-recovery current in the Si diode occurs before the voltage rises. This indicates that charge storage is far more important than junction capacitance in the Si diode. Fig. 5 shows a reverse-recovery comparison between an ultrafast 600-V Si p-i-n diode (BYV26V) and this 1200-V SiC JBS diode. The reverse-recovery current in the Si diode is huge in comparison to that of the SiC diode. Furthermore, the nature of the charge storage-type recovery for the Si diode means that the anti-parallel switch (e.g., IGBT, MOSFET, or CoolMOS™) in a hard-switched power converter experiences the full supply voltage at full current (load current plus diode current) during the switch turn-on. In contrast, the anti-parallel switch experiences less voltage during turn-on with the SiC JBS diode because the voltage begins to rise at the beginning of the diode recovery.

2) Efficiency Measurements: A 50-W buck converter power supply circuit was designed for a 500 V–100 V step-down application. This test circuit used a CoolMOS™ transistor for the switch. With conventional ultrafast reverse-recovery diodes, the switching frequency is limited. In initial testing, several commercially available ultrafast Si diodes were destroyed at 100 kHz switching because of excessive diode reverse-recovery associated losses. These losses lead to overheating of the devices due to excessive heating, even when operated within their specified current levels. The final comparison can only be applied to the SiC JBS diode rated at 1200 V, 0.5 A and the BYV26C Si diode, rated at 600 V, 1 A. Fig. 6 shows the results of the efficiency model and measurements at 186 kHz switching frequency. Both modeling and experimental results indicate that the system efficiency with the SiC JBS diode is between 87% and 89% for most load conditions. By comparison, the system efficiency with the BYV26C Si diode varies between 81% and 85% under the same load conditions. Fig. 7 compares the loss distribution between the systems with SiC JBS and the BYV26C Si diodes at 100 kHz switching. The loss model includes five loss components: 1) diode conduction ($D_{\rm con}$); 2) device conduction ($Q_{\rm on}$); 3) turn-on switching ($SW_{\rm on}$); 4) turn-off switching ($SW_{\rm off}$); and 5) diode reverse-recovery (D_{rr}). The I^2R loss associated with the power supply inductor is included in the efficiency evaluation. With the Si diode, the most dominant loss component is the turn-on switching loss in the switch. With the same switching device, the turn-on loss can be significantly reduced with a faster reverse-recovery diode. In this example, the SiC JBS diode reduces the turn-on loss over the ultrafast Si p-i-n diode by more than 40%.

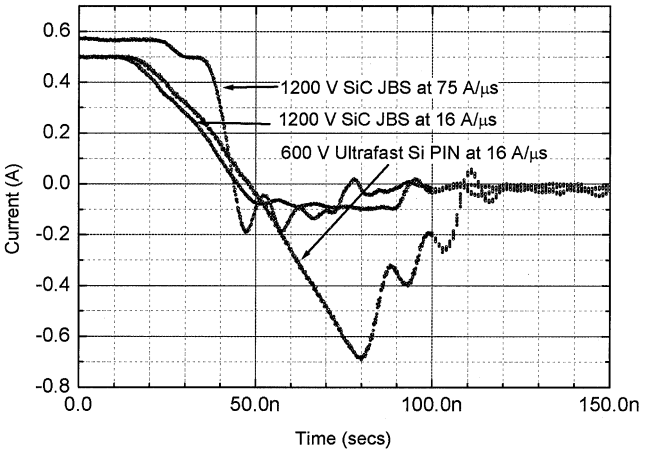

Fig. 5. Reverse-recovery waveforms comparing 600-V ultrafast Si p-i-n and 1200-V SiC JBS diode at reverse dI/dt of 16 A/μs. No reverse-recovery current is observed in the JBS diode even at a reverse dI/dt of 75 A/μs.

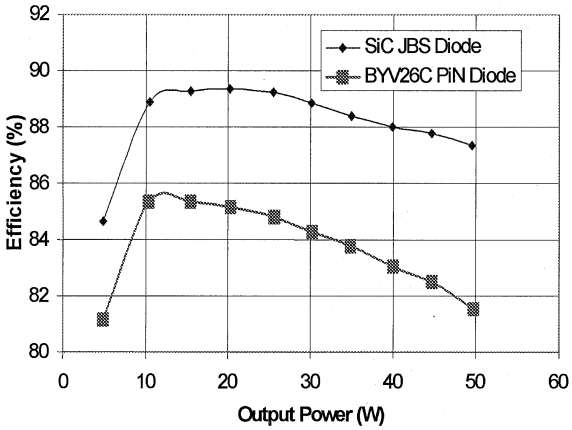

Fig. 6. DC/DC converter made using 600-V CoolMOS™ shows a 6% increase in conversion efficiency with a 1200-V SiC JBS diode as compared to the fastest 600-V Si diode at an operating frequency of 186 kHz.

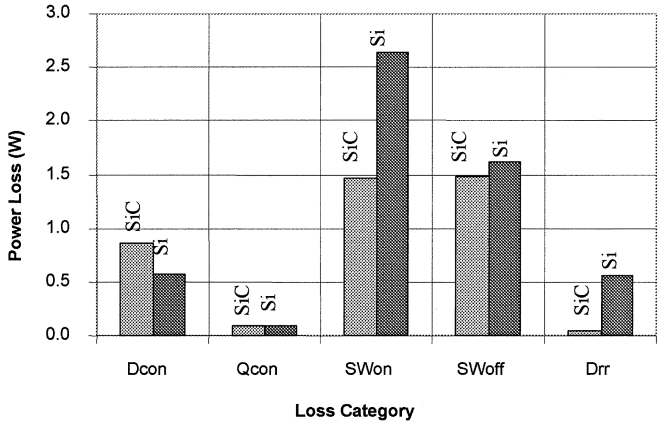

Fig. 7. Comparison of Si and SiC power loss components of a dc/dc converter.

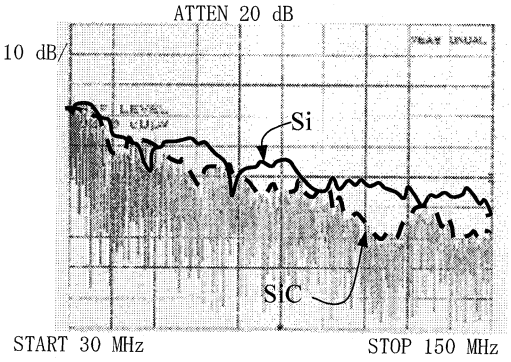

Fig. 8. Comparison of EMI spectrum envelope for the switching power supply with Si and SiC diodes.

3) EMI Measurements: The diode reverse-recovery has been considered as the major source of EMI. With nearly zero reverse-recovery time, the SiC JBS diode is expected to emit less EMI high-frequency noise. Experiments were conducted to compare the EMI performance of the above-mentioned converter using both BYV26C Si and SiC JBS diodes. Fig. 8 shows the experimental EMI spectrum for the frequency range 30 MHz–150 MHz. For comparison purposes, the EMI spectrum of the Si diode is only shown with the envelope. The major EMI reduction with the SiC diode appears in the frequency range 70 MHz–150 MHz.

IV. Optimized High-Power JBS Diodes

A. Design and Fabrication of Second Batch of JBS Diodes

Based on the results obtained from the JBS diodes reported in the previous sections, a new layout design of higher current JBS diodes was implemented. The new mask set had 3 mm $\times$ 3 mm diodes, which can be expected to carry four times higher current as compared to the largest diodes fabricated in the previous batch. These diodes had the same epitaxial design, i.e., 20 μm of 2E15 cm^{-3} voltage-blocking layers. As reported earlier, the most appropriate layout grid design for this voltage range was found to be the linear design with a Schottky region width of 4 μm and the implanted p$^+$ region of 2 μm, which was implemented in this batch of devices. The fabrication sequence of these JBS diodes was similar to those reported for the previous batch of devices. The steps required for the fabrication of p-i-n diodes on the same wafer were omitted. As-deposited nickel was used as the Schottky metal and annealed Nickel was used as the backside ohmic contact.

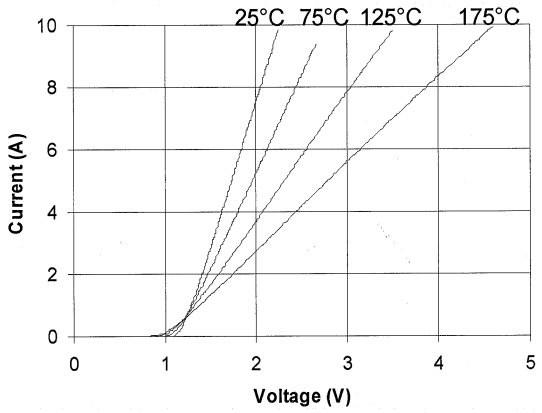

Fig. 9. Measured temperature dependence of the on-state voltage for 3 mm $\times$ 3 mm 4H-SiC JBS diode.

B. Static Characteristics

The measured temperature dependence of the on-state characteristics for a 3 mm $\times$ 3 mm SiC JBS diode is shown in Fig. 9. For this diode, the on-state voltage drop at 20 A (225 A/cm^2) was 3.1 V, which corresponds to a specific on-resistance of 8.5 mΩ-cm^2 . These characteristics were obtained on "best few" devices from this lot. The increase in on-state voltage with respect to temperature is indicative of the reduction in electron mobility with increasing temperature for a majority carrier device. Although this positive temperature coefficient of resistance increases the on-state loss at high temperatures, it is beneficial for paralleling and large-area current sharing. These large-area diodes showed a blocking voltage of 1410 V, as seen from the reverse I–V characteristics of Fig. 10. On smaller, 1.5 mm $\times$ 1.5 mm 4H-SiC diodes fabricated alongside these large-area diodes, a blocking voltage of 1900 V was obtained. The higher blocking voltage on smaller devices was probably due to a lower probability of finding material and process defects. The on-state J–V characteristics of both of these diodes were nearly identical.

C. Switching Characteristics in Hard-Switching Applications

Fig. 11 shows a hard-switching chopper test circuit. The circuit consists of two branches of switch-diode pairs. Both switches S_1 and S_2 are turned ON and OFF simultaneously. Diodes D_1 and D_2 provide a freewheeling path when both switches are turned OFF. Such a chopper has been widely used in magnetic levitation, magnetic bearing, and switched reluctance motor drives. The bottom devices served as the devices under test (DUT) and the current measurement was implemented with low-inductance current-sensing resistors R_D and R_S. Major circuit components used in this circuit are listed as: S_1, S_2: 600-V, 20-A MOSFET; D_1, D_2: 600-V, 20-A fast recovery Si diode, or alternatively for comparison, the above-mentioned SiC JBS diode; and L: 2 mH. The measured switch voltage and current were: S_2 drain-source voltage, v_S; source current, i_S; D_1 cathode-anode voltage, v_D; and anode current, i_D. A 300-V bus voltage was used in this hard-switching circuit.

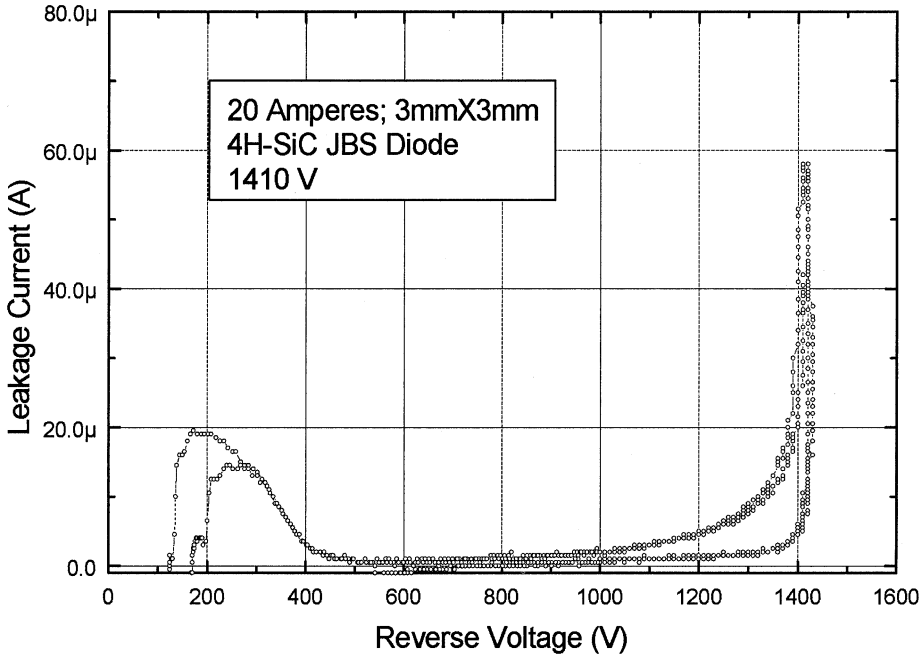

Fig. 10. Measured reverse $I-V$ characteristics of 3 mm × 3 mm 4H-SiC JBS diode.

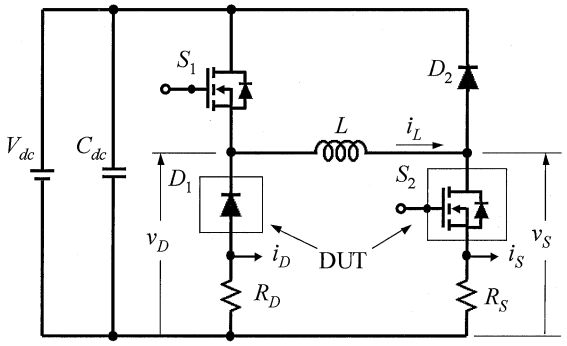

Fig. 11. Circuit diagram of hard-switching chopper.

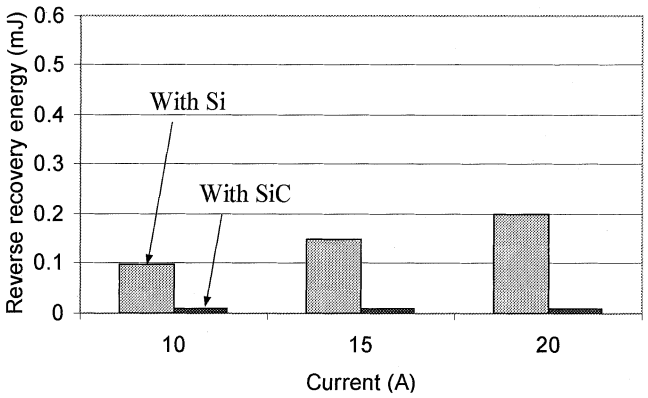

Fig. 12. Reverse-recovery energy of SiC JBS diode and a fast Si diode under different load conditions in a hard-switching chopper circuit.

1) Diode Reverse-Recovery Characteristics: With the Si diode, the reverse-recovery time t_{rr} was about 160 ns and the peak reverse-recovery current $I_{D\text{-}rr}$ was 30 A, or 1.5 times the load current I_L. With the SiC JBS diode, the reverse-recovery time (which was primarily capacitive) was about 80 ns and the peak reverse current was 10 A, or half the load current. Once the switching device voltage reaches its on-state value, the diode current starts returning to zero and the switching loss due to this part of the diode reverse-recovery can be expressed as: $P_{D\text{-}rr} = f_{sw} \cdot E_{D\text{-}rr,}$, where $E_{D\text{-}rr}$ is the diode switching energy associated with the diode reverse-recovery. Fig. 12 shows the diode reverse-recovery energy $E_{D\text{-}rr}$ of the SiC JBS diode and the Si diode under different load conditions. With the Si diode as the DUT, the $E_{D\text{-}rr}$ is 0.2 mJ at a 20-A load condition. With the SiC diode as the DUT, the $E_{D\text{-}rr}$ is 0.02 mJ at a 20-A load condition. The energy loss with the Si diode is a function of the load current. However, the energy loss with the SiC diode during the reverse-recovery period tends to be constant over the entire load range. This indicates that the small amount of energy loss or the intersection of voltage and oscillating current is likely caused by the parasitic components, but not the reverse-recovery.

2) Switch Turn-On and Turn-Off Characteristics: From the turn-on current and voltage waveforms of the MOSFET at a 300-V bus voltage and 20-A load current condition, the losses in the switch can be analyzed in this circuit in a realistic application. The switch current i_S contains the load current and the diode reverse-recovery current. With the Si diode, a 27-A current overshoot is observed, along with parasitic ringing associated mainly with the sensing resistor for the measurement. With the SiC diode, i_S contains negligible overshoot, but parasitic ringing similar to that with the Si diode remains. The turn-on energies E_{on} of the main switches S_1 and S_2 are influenced by the reverse-recovery of the freewheeling diodes D_1 and D_2. With a nearly zero reverse-recovery characteristics, the SiC JBS diode significantly reduces the switch turn-on energy as compared to the Si diode counterpart. Fig. 13 compares the turn-on energy of S_2. With the Si diode as the freewheeling diode D_2, the turn-on energy is 1.5 mJ at the 20-A load condition; while with the SiC diode as the freewheeling diode, E_{on} is 0.4 mJ at the 20-A load condition. Thus, the use of SiC JBS diodes reduces the switch turn-on related losses by more than 70%.

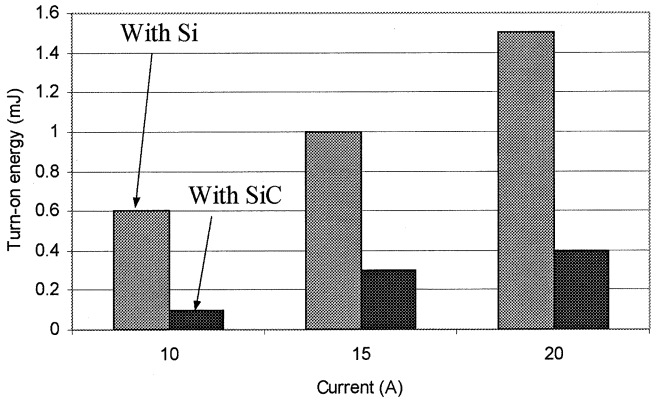

Fig. 13. Turn-on energy of a MOSFET with either a SiC JBS diode or an ultrafast Si diode under different load currents.

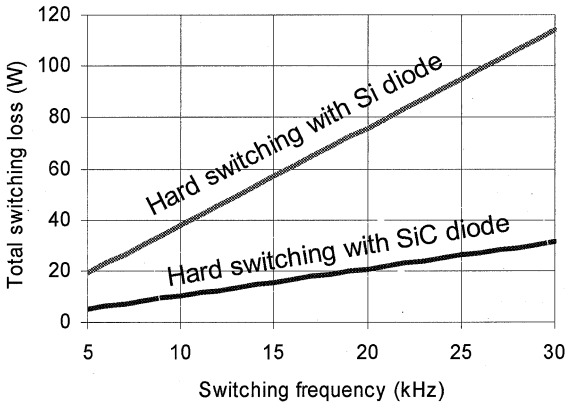

Fig. 14. Comparison of the total switching loss as a function of switching frequency for a 6-kVA chopper using Si and SiC JBS diodes.

The turn-off energy of the MOSFET is invariant whether the freewheeling diode is Si or SiC JBS. At a 20-A load current, the turn-off energy E_{off} is 0.2 mJ using either diode. Based on the switching energy obtained above, the total switching losses using the SiC JBS diode and the fast Si diode can be compared. The total device switching loss for each switch pair can be expressed as $P_{Q\text{-}sw} = f_{sw}(E_{\text{on}} + E_{\text{off}})$ and the diode reverse-recovery loss can be expressed as $P_{D\text{-}rr} = f_{sw} \cdot E_{D\text{-}rr}$, where f_{sw} is the switching frequency. Fig. 14 compares the total switching losses ($= 2P_{Q\text{-}sw} + 2P_{D\text{-}rr}$) for a chopper using the SiC JBS diode and the fast Si diode under different switching frequencies. The calculation here is for a 6-kVA chopper with a bus voltage of 300 V and a load current of 20 A. It can be seen that the use of a SiC JBS diode cuts switching losses more than 60%, thus dramatically reducing size and cooling requirements.

D. Switching Characteristics in Soft-Switching Applications

Fig. 15 shows the soft-switching test circuit using an auxiliary resonant snubber chopper (ARSC). The basic circuit structure is similar to that shown in Fig. 11 with two main switches S_1 and S_2 and two main freewheeling diodes D_1 and D_2. The lossless snubber capacitors are connected across the main switches and diodes. With soft-switching, the main diode can have a slow reverse-recovery [10]. An auxiliary resonant circuit that consists of an auxiliary switch S_r, diode D_r, and resonant inductor L_r is connected across the middle points of the two chopper legs. With proper resonant circuit design and control timing, this type of converter can achieve near-zero voltage turn-on and avoid the loss due to diode reverse-recovery [9], [10]. In terms of switching timing, the gating signals of the main devices with a fixed time period corresponding to the desired load current is the same as that used in the hard-switching test circuit. The gate signal of the auxiliary switch is added before the main switch is turned on to ensure zero voltage turn-on of S_2. The basic operating principle of the zero voltage switching for this ARSC test circuit is described in detail in [10] and [11]. The major advantage of this soft-switching operation over conventional hard-switching operation is to provide a zero voltage condition before the MOSFET turns on. The MOSFET turn-off voltage is snubbed by the capacitors across the main devices.

The main problem with this circuit operation is the reverse-recovery of the auxiliary branch diode D_r. When the resonant

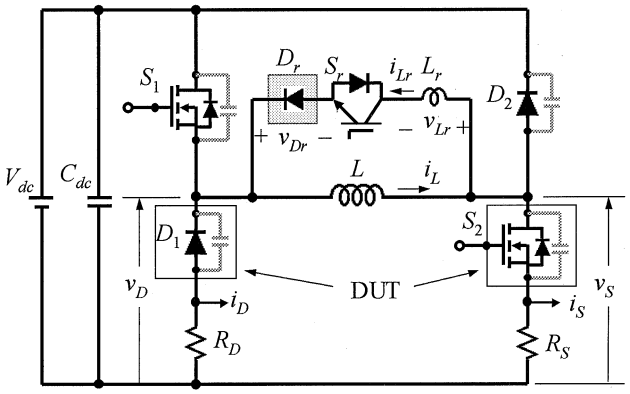

Fig. 15. Auxiliary resonant snubber chopper test circuit for soft-switching.

current drops to zero and is blocked by D_r, the reverse-recovery current creates an oscillation, which induces an over voltage condition for the auxiliary diode. From the experimental results using one of the best available ultrafast reverse-recovery Si diodes, rated at 50 A and 600 V as the auxiliary diode, this circuit was analyzed for total efficiency. Voltage and current waveforms show that the diode turns off naturally as i_{Lr} goes to zero, with a small reverse-recovery current. The reverse-recovery current follows a parasitic ringing that is caused by the junction capacitance of the diode and the resonant inductance and this introduces a large reverse voltage peak on the diode, which is more than twice the dc bus voltage. In this case, the dc bus voltage was 200 V and the voltage peaked at 420 V. For a 300-V dc bus voltage and with a 600-V device rating, this soft-switching circuit with this Si diode simply cannot be operated without exceeding the diode rating.

To reduce the ring excitation effect of the reverse-recovery of the auxiliary resonant branch diode, it is common to add an RC snubber across the switch to reduce the voltage rise rate and peak voltage or a saturable reactor (SR) in series with the inductor so that the diode current can be turned off with a greatly reduced dI/dt slope. The SR causes the effective inductance of L_r to become large as the current nears zero at the point of diode recovery. This phenomenon can be seen from the i_{Lr} waveform. With the slow falling rate of the resonant current, the peak diode voltage is reduced to 350 V. This approach has been widely used in many soft-switching circuits to resolve the

diode reverse-recovery problem that has been hindering the use of the zero voltage switching inverter. The result indicates that overshoot voltage is reduced to less than 20%. The use of the SR is not without problems with a non-trivial switching energy of 0.5 mJ associated with the SR. If the switching frequency is 20 kHz, the SR consumes 10 W. This additional loss not only reduces the system efficiency, but also causes difficulties with cooling and packaging a small footprint magnetic core. With a total switching loss of about 60 W, the SR loss represents more than 16% of the total loss.

To avoid the use of the SR, or other voltage clamping means, the reverse-recovery of the auxiliary diode must be fully eliminated. This prompts the use of the SiC JBS diode to eliminate reverse-recovery and thus to reduce the voltage overshoot. From the experimental voltage and current waveforms using the high-current SiC JBS diode with the 300-V DC bus, the diode reverse-recovery is reduced. However, the diode junction capacitance tends to ring with the resonant inductor and results in a voltage spike about 45% higher than the dc bus voltage. As compared to the circuit with the Si diode, the voltage overshoot is largely reduced and a 600-V device can be comfortably used in a 300-V dc bus system with the SiC diode. More importantly, the circuit does not need the SR, or other voltage clamping means and additional associated losses and costs are eliminated. It should be noted that this 3 mm $\times$ 3 mm SiC JBS diode operates at 39 A peak resonant current quite comfortably. The diode turns ON and OFF under zero current conditions and the only loss comes from the on-state voltage drop. Fortunately, the auxiliary diode conduction period is only 1.5 μs over a 50-μs period. The diode conduction loss is less than 1 W for the 6-kVA system and its body temperature can be maintained near room temperature without heat sinking.

To demonstrate the advantage of the SiC JBS diode in soft-switching applications, the turn-on loss comparison is made for the following three cases in Fig. 16.

Case 1) hard-switching chopper with the Si diode;
Case 2) soft-switching chopper with the Si diode and the SR in the auxiliary resonant circuit;
Case 3) soft-switching chopper with the SiC JBS diode in the auxiliary resonant circuit.

For a 6-kVA chopper operating at a 20-kHz switching frequency, the use of the SiC JBS diode, or Case 3, cuts the turn-on loss of the soft-switching chopper by more than 50% as compared to the use of a ultrafast reverse-recovery Si diode and SR, or Case 2. As compared to the hard-switching chopper, or Case 1, the use of the SiC JBS diode cuts the turn-on loss from 52 W to 8 W, about an 86% percent loss reduction.

V. Summary

Detailed design, fabrication, and characterization of 1500-V, 4-A 4H-SiC JBS diodes are presented. Two-dimensional simulations show that for a Schottky region spacing of 4 μm, the electric field at the Schottky contact is only 62% of the peak electric field in the device. Diodes with a linear p^+ grid JBS shows slightly better performance than a honeycombe JBS diode. JBS diodes show on-state and switching characteristics similar to Schottky diodes and blocking characteristics similar

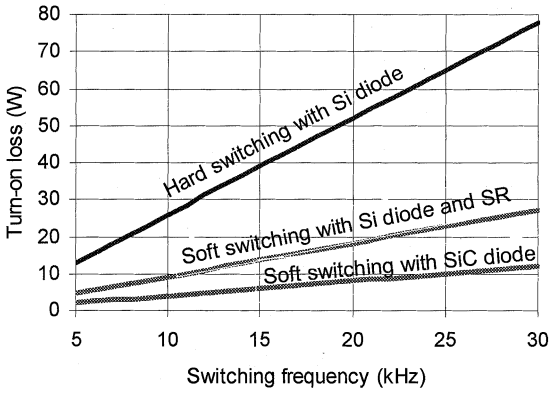

Fig. 16. Turn-on loss comparison for three different cases in a soft-switching circuit.

to p-i-n diodes. Measurements on 0.0045 cm^2, 1200-V, 0.5-A 4H-SiC JBS diodes indicate that the reverse-recovery time and associated losses are near zero even at a reverse dI/dt of 75 A/μs. Based on measured waveforms, detailed loss models on diode switching were established for a high-frequency switching power supply efficiency evaluation. A 600-V CoolMOS™ was used to compare the conversion efficiency of a dc/dc converter circuit with a 600-V ultrafast Si diode and a 1200-V SiC JBS diode. At about 200 kHz switching, the power supply efficiency improvement was about 6%, over the fastest, lower blocking voltage Si diode. EMI measurements indicate smaller signatures as compared to those observed for Si diodes in a dc/dc converter.

Higher current SiC JBS diodes in both hard-switching and soft-switching circuits were also evaluated. Experimental results indicate that in hard-switching applications the use of the SiC JBS diode almost eliminates the reverse-recovery and the associated transistor turn-on current overshoot as compared to its Si diode counterpart, thus reducing the transistor turn-on losses more than 70%. In soft-switching applications, the use of a SiC JBS diode in the auxiliary branch reduces voltage ringing by more than 50% compared to the ringing caused by the recovery of an ultrafast Si diode. With the Si diode, the ringing is too high to allow the auxiliary branch network to be used without special suppression techniques such as snubbers or SRs. When compared with the use of the Si diode and SR, the use of the SiC diode reduces the power loss associated with the auxiliary branch by 50%. Compared to hard-switching, the use of the JBS SiC diode in the soft-switching circuit can reduce transistor turn-on losses more than 86%. These rectifiers are expected to result in the advent of a new generation power hardware with dramatically increased capabilities.

References

[1] R. Held, N. Kaminski, and E. Niemann, "SiC merged pn/Schottky rectifiers for high-voltage applications," in *Mater. Sci. Forum*, vol. 264–268, 1998, pp. 1057–1060.
[2] F. Dahlquist, C. M. Zetterling, M. Ostling, and K. Rottner, "Junction barrier Schottky diodes in 4H-SiC and 6H-SiC," in *Mater. Sci. Forum*, vol. 264–268, 1998, pp. 1061–1064.
[3] P. Alexandrov, J. H. Zhao, W. Wright, M. Pan, and M. Weiner, "Demonstration of 140 A, 800 V 4H-SiC p-i-n/Schottky diodes with multistep junction termination extension structures," *Electron. Lett.*, vol. 37, pp. 1139–1140, Aug. 2001.

[4] ——, "Inductively loaded half-bridge inverter characteristics of 4H-SiC merged p-i-n/Schottky diodes up to 230 A and 250 °C," *Electron. Lett.*, vol. 37, pp. 1261–1262, Sept. 2001.
[5] C. M. Johnson, N. G. Wright, A. B. Horsfall, D. J. Morrison, M. Rahimo, D. A. Hinchley, and A. Knights, "Characterization of 4H-SiC Schottky diodes for IGBT applications," in *Conf. Rec. IEEE IAS Annu. Meeting*, Roma, Italy, 2000, pp. 2941–2947.
[6] A. R. Hefner, Jr., D. W. Berning, J.-S. Lai, C. Liu, and R. Singh, "Silicon carbide merged p-i-n Schottky diode switching characteristics and evaluation for power supply applications," in *Conf. Rec. IEEE IAS Annu. Meeting*, Roma, Italy, 2000, pp. 2948–2954.
[7] J.-S. Lai *et al.*, "A delta configured auxiliary resonant snubber inverter," *IEEE Trans. Ind. Applicat.*, no. 3, pp. 518–524, 1996.
[8] W. McMurray, "Resonant snubbers with auxiliary switches," *IEEE Trans. Ind. Applicat.*, vol. 29, no. 2, pp. 355–362, 1993.
[9] J. S. Lai, "Fundamentals of a new family of auxiliary resonant snubber inverters," in *Conf. Rec. IEEE IECON*, Nov. 1997, pp. 645–650.
[10] B. M. Song and J.-S. Lai, "A novel two-quadrant soft-switching converter with one auxiliary switch for high-power applications," *IEEE Trans. Ind. Applicat.*, no. 5, pp. 1388–1395, 2000.
[11] H. Yu, B.-M. Song, and J.-S. Lai, "Design of a novel ZVT chopper," *IEEE Trans. Power Electron.*, vol. 17, pp. 101–108, Jan. 2002.

Ranbir Singh recieved the B.Tech degree from Indian Institute of Technology, New Delhi, in 1990, and the M.S. and Ph.D. degrees from North Carolina State University, Raleigh, in 1992 and 1997, respectively, all in electrical engineering. His graduate experience included exposure to a wide variety of both bipolar and MOS families of devices, with his specialty in characterizing the cryogenic operation of Si power devices.

Since August 1995, he has been with Cree, Inc., Durham, NC, where he conducts research on SiC power devices. His interests include development of SiC power MOSFETs, IGBTs, field-controlled thyristors, JBS, and p-i-n and Schottky diodes. He has co-authored over 60 publications in various refereed journals and conference proceedings and is an inventor on 12 issued U.S. patents. He has made two invited MRS presentations in 2000 and 2002. He served on the technical committee of the International Symposium on Power Semiconductor Devices and ICs (ISPSD) in 2002 and 2003, and was part of a panel to develop a roadmap for the insertion of SiC-based power devices into commercial applications. He is the author of the book *Cryogenic Operation of Silicon Power Devices* (Norwell, MA: Kluwer, 1998).

D. Craig Capell received the A.A.S. degree in electronic engineering technology from Durham Technical College, Durham, NC in 1988.

He has been developing novel semiconductor processsing techniques for power and microwave devices made using advanced wide band gap semiconductors like SiC and GaN. Since joining Cree, Inc., Durham, in 1993, he has been primarily responsible for process optimization of power FETs, power rectifiers, and microwave FETs in the Advanced Device Fabrication Laboratory. These processing techniques include reactive ion etching for fast and accurate etching of SiC and GaN, novel MOS processing for high-channel mobilities, advanced metallization for wide band gap Schottky rectifiers, and passivaton stacks for ultra-high-voltage devices. He has optimized photolithography techniques for achieving extremely small linewidths. He was responsible for the process optimization and extending the voltage and current ratings of high-power JBS and p-i-n rectifiers, UMOSFETs, ACCUFETs, BJTs, GTOs, FCTs, and Schottky diodes. ¸Prior to joining Cree, Inc., he was involved with process development and project leadership roles with Harris Semiconductor, Melbourne, FL, as well as GE Semiconductor, Research Triangle Park, Durham.

Allen R. Hefner (S'83–M'84–SM'93–F'01) was born in Washington, DC, on June 29, 1959. He received the B.S., M.S., and Ph.D. degrees in electrical engineering from the University of Maryland, College Park, in 1983, 1985, and 1987, respectively.

He joined the Semiconductor Electronics Division of the National Institute of Standards and Technology (NIST), Gaithersburg, MD, in 1983. He is presently the Group Leader for the NIST Semiconductor Electronics Division's Device Technology Group. His research interests include characterization, modeling, and circuit utilization of power semiconductor devices and MEMS-based integrated sensor system-on-a-chip technologies.

Dr. Hefner was elected as an IEEE Fellow for contributions to theory and modeling of power semiconductor devices in 2001. In 1993, he received a U.S. Department of Commerce Silver Metal Award for his pioneering work in modeling advanced power semiconductor devices for electro-thermal circuit simulation. He is also the recipient of the 1996 NIST Applied Research Award for development and transfer of the IGBT model to circuit simulator software vendors, and an IEEE Industry Applications Society Prize Paper Award. He is the author of 60 publications in IEEE TRANSACTIONS and conference proceedings. He has presented 30 invited seminars and was an Instructor for the IEEE Power Electronic Specialist Conference tutorial course (1991 and 1993) and for the IEEE Industry Applications Society Meeting tutorial course (1994). He has served as a Program Committee Member for the IEEE Power Electronics Specialist Conference (1991–1999) and the IEEE International Electron Devices Meeting (2001), and as the Transactions Review Chairman for the IEEE Industry Applications Society Power Electronics Devices and Components Committee (1989–1997). He has also served as the IEEE Electron Devices Society Standards Technical Committee Chairman (1996–2001) and is a Member of the IEEE Electron Devices Society Power Devices and Integrated Circuits Technical Committee and the IEEE Power Electronics Society Technical Committee for Computers in Power Electronics.

Jason Lai (S'89) received the M. S. and Ph.D. degrees in electrical engineering from the University of Tennessee, Knoxville, in 1985 and 1989, respectively.

From 1980 to 1983, he was the Head of the Electrical Engineering Department of the Ming-Chi Institute of Technology, Taipei, Taiwan, R.O.C., where he initiated a power electronics program and received a grant from his college and a fellowship from the National Science Council to study abroad. In 1986, he became a Staff Member at the University of Tennessee, where he taught control systems and energy conversion courses. In 1989, he joined the Electric Power Research Institute (EPRI) Power Electronics Applications Center (PEAC), where he managed EPRI-sponsored power electronics research projects. In 1993, he joined the Oak Ridge National Laboratory as the Power Electronics Lead Scientist, where he initiated a high-power electronics program and developed several novel high-power converters including multilevel converters and auxiliary resonant snubber-based soft-switching inverters. Since August 1996, he has been with the Virginia Polytechnic Institute and State University, Blacksburg, as an Associate Professor. His main research areas are in high-power electronics converter topologies, motor drives, and utility power electronics interface and application issues. He has published more than 100 technical papers and two books. He received eight U.S. patents in the area of high-power electronics and their applications.

Dr. Lai is Chairman of the IEEE Power Electronics Society Standards Committee. He chaired the Technical Committee for the 2001 DOE Future Energy Challenge. He has been the recipient of several distinctive awards including a Technical Achievement Award in Lockheed Martin Award Night, two IEEE IAS Conference Paper Awards from Industrial Power Converter Committee, one IEEE IECON Best Paper Award, and an Advanced Technology Award from Inventors Clubs of America.

John W. Palmour (M'95) received the B.S. and Ph.D degrees from North Carolina State University, Raleigh, in 1982 and 1988, respectively. His major was in materials science and engineering, with a minor in electrical engineering. His doctoral research concentrated on processing techniques and transistor development in SiC, and he demonstrated a SiC MOSFET operating at 650 °C.

He became a Co-founder of Cree, Inc., Durham, NC, where he is the Director of Advanced Devices. He has been responsible for the development of high-voltage, high-temperature 4H-SiC power diodes, MOSFETs, and thyristors, as well as high-frequency SiC MESFETs and planar n-channel and p-channel 6H-SiC MOSFETs. He is also responsible for Cree's development of microwave GaN HEMTs. He has coauthored over 175 publications in various conference proceedings and refereed journals, and is an inventor on 17 issued U.S. patents concerning semiconducting SiC. He also serves on the Board of Directors for Cree, Inc.